P2B.9

APPLICATION OF THE RAIN PROFILING ALGORITHM "ZPHI" TO THE X-BAND POLARIMETRIC RADAR DATA OBSERVED IN JAPAN

Koyuru Iwanami*[1], Erwan Le Bouar[2], Jacques Testud[2],
Masayuki Maki[1], Ryohei Misumi[1], Sang-Goon Park[1] and Mihoko Suto[1]
1: National Research Institute for Earth Science and Disaster Prevention (NIED), Tsukuba, Japan
2: Centre d'Étude des Environnements Terrestre et Planétaires (CETP), Vélizy, France

1. INTRODUCTION

It is so important to estimate rain rate accurately for not only investigation of precipitation systems but also mitigation of disasters related to heavy rainfall such as floods and shallow landslides. Z-R relationship has been used for rain rate estimation extensively but it is well known that the Z-R relationship is seriously affected by variability of raindrop size distributions. Recently polarimetric technique made it possible to use the specific differential propagation phase K_{DP} for quantitative rain rate estimates. X-band radars are revalued because they have better sensitivity of K_{DP} for light rain than S- and C-band radars although they have not been thought to be appropriate for the operational use because of strong attenuation by rain.

We applied the rain profiling algorithm ZPHI developed by Testud et al. (2000) to the rainfall observation data by the NIED X-band polarimetric radar (MP-X) and compared estimated rain rates from ZPHI algorithm with the disdrometer measurements and estimation results by the other methods.

2. ZPHI ALGORITHM

ZPHI algorithm has been developed for dual polarization radars in attenuating frequencies (Testud et al., 2000). ZPHI is a rain profiling algorithm that uses the profile of measured reflectivity and $\Delta\Phi$ of difference of differential propagation phase Φ_{DP} measurements in a segment between two selected range bounds as a constraint. It is basically assumed that the normalized intercept parameter of raindrop size distribution N_0^* (Testud et al., 2001) is constant in the segment. This hypothesis is reasonable when the interval is covering a unique kind of rain. Consequently ZPHI operates a systematic segmentation along each ray so as to ensure an optimal variability of N_0^*, that is, constant in each interval but variable along the segmented ray.

The primary output parameters are the specific attenuation A in dB km^{-1} and N_0^* in m^{-4}. The rain rate R mm h^{-1} is deduced by the following equation:

$$R = pN_0^{*(1-q)}A^q, \qquad (1)$$

where p and q are coefficients depending on temperature and elevation angle. For example, p = 1.66 and q = 0.756 at temperature T = 10 C and 0 deg elevation in X-band frequency (Le Bouar et al., 2002). ZPHI is also capable to correct differential reflectivity Z_{DR} for attenuation utilizing a power low relationship between specific differential attenuation A_{DP} and A.

* *Corresponding author address:* Koyuru Iwanami, National Research Institute for Earth Science and Disaster Prevention (NIED), 3-1 Tennodai, Tsukuba, 305-0006 JAPAN; e-mail: iwanami@bosai.go.jp

3. OBSERVATION AND DATA

NIED carried out the field experiment of "Real Time Dual Doppler Radar Experiment 2001 (DDX01)" using two X-band, a Ka- and a W-band Doppler radars, a microwave radiometer and three impact type disdrometers (RD-69; Distromet Co. Ltd.) from August 8 to October 4 in 2001 around Tsukuba city, Japan. One of the main purposes of this experiment was collecting basic data to develop and validate measurement and estimation techniques of cloud and rain by multiparameter radars such as rain rate estimation using differential propagation phase.

The radar data by X-band multiparameter radar (MP-X; Iwanami et al., 2001) and raindrop size distribution data by three impact type disdrometers were used for this study. Main specifications of the MP-X radar are listed in Table 1.

TABLE 1 Main specifications of MP-X

Frequency	9.375 GHz
Antenna Type	Circular Parabola, 2.1m$^\Phi$
Scan Range (Rate): AZ	Full Circle (≤ 36 deg s^{-1})
EL	-2 to +92 (≤ 18 deg s^{-1})
Antenna Gain	41.6 dB
Beam Width	1.3 deg
Transmitter Tube	Magnetron
Peak Power	50 kW
Pulse Length	0.5 µs
PRF	≤ 1,800 Hz
Polarization	H & V
Doppler Processing	PPP, FFT
Noise Figure	2.3 dB
Observation Range	80 km
Outputs	Z, V, W, Z_{DR}, ρ_{hv}, Φ_{DP}, K_{DP}

MP-X collected data continuously by sets of a PPI scan of elevation angle of 2.5 deg and an RHI scan of azimuth angle of 294.0 deg in the direction of three disdrometer sites every about 2 min 20 sec. The pulse repetition frequency, number of sampling pulses and data resolution in scanning angle was selected 1,800 Hz, 256 and 0.5 deg, respectively, and then the rotation speed of the antenna became 3.5 deg sec^{-1}.

Three disdrometers were set up on the one line to examine algorithms for attenuation correction and rain rate estimation (see Fig. 1) and their data were recorded every one minute.

Estimation of calibration correction of radar reflectivity Z dBZ and differential reflectivity Z_{DR} dB was carried out first. Radar reflectivity values in vertically pointing measurements by MP-X at 500 m range were compared with estimated reflectivity from raindrop size distributions measured by disdrometer on June 21, 2001 using T-matrix method (Bringi et al., 1990). The calibration correction of reflectivity Z was estimated to be -6.4 dBZ from this comparison. The bias of differential reflectivity Z_{DR} of MP-X was estimated by using vertically pointing but azimuthally scanning measurements by the method of Gorgucci et al. (1999). The value of +1.38 dB of calibration correction was resulted from collected data from 2.2 to 3.9 km height in rain region for 18 minutes on October 1, 2001.

After unfolding of differential propagation phase Φ_{DP} deg, MP-X data were transformed to the input data format for ZPHI calculation. The MP-X data nearer than 2 km range were not used for ZPHI calculation because erroneous data were included in this range.

4. RESULTS

The analyses were carried out for the rainfall case from 01 to 03 JST (Japan Standard Time) on September 11 in 2001 when the maximum rain rate of 121 mm h^{-1} was recorded on the ground by a disdrometer at the site of YMTO. A series of rainfall was accompanied by a rain band associated with the Typhoon T0115. A PPI image of reflectivity Z before bias correction with range of 40-km by MP-X is shown in Fig. 1. The rain band moved from south-southeast to north-northwest in about 65 km h^{-1} and passed over the radar site about 02:04 JST. Strong attenuation effect of heavy rainfall can be seen behind the rain band.

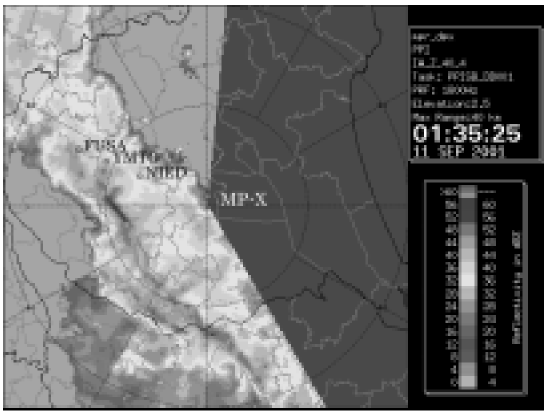

FIG. 1. PPI image of reflectivity of 2.5 deg elevation. The locations of three disdrometer sites are shown by small squares with site names. MP-X collected data from 150 to 5 deg in azimuth.

4.1 Results of ZPHI Calculation on One Ray

ZPHI calculation operates on a ray-by-ray basis. Figure 2 illustrates a result of application of ZPHI algorithm to a ray of azimuth angle of 294.1 deg on disdrometer sites on 2.5 deg PPI data at 02:02:10 JST. Altitude of freezing level was 5.1 km by the upper air sounding, then it was expected that radar beam sampled rain medium at this elevation within the full range of 80 km because there was no report of hail in this period.

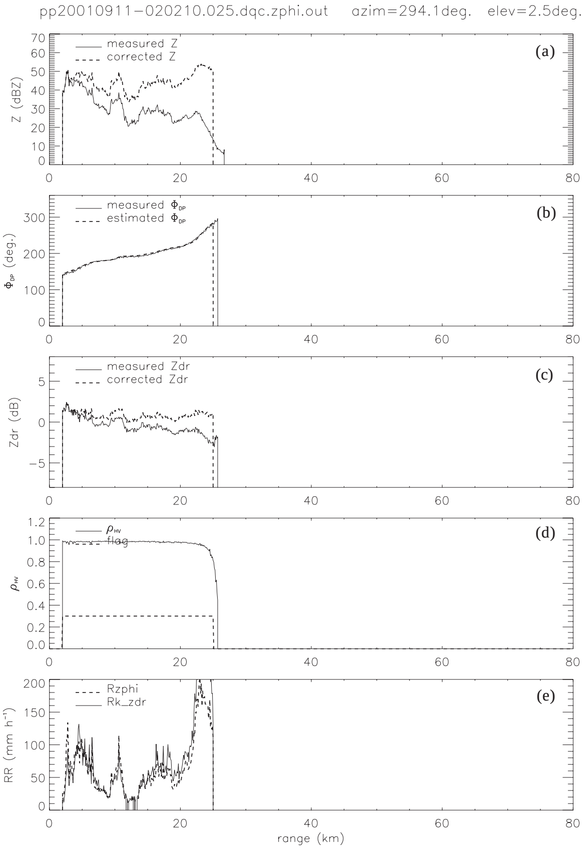

FIG. 2. Profiles of (a) measured (solid line) and corrected (broken line) reflectivity Z, (b) measured (solid) and model adjusted (broken) differential propagation phase Φ_{DP}, (c) measured (solid) and corrected (broken) differential reflectivity Z_{DR}, (d) measured correlation coefficient ρ_{hv} (solid) and ZPHI calculation flag (broken), (e) retrieved rain rate from ZPHI (broken) and both specific attenuation A and Z_{DR} (solid) along the ray of 2.5 deg elevation and 294.1 deg azimuth at 02:02:10 JST on Sep. 11, 2001.

ZPHI calculation flag in Fig. 2(d) shows index of 3 (values with the ordinate are needed to be increased by ten times for the flag) that means the full ZPHI version was operated and calculation quality was good from 2 to 25 km range. The profile of estimated differential propagation phase Φ_{DP} in Fig. 2(b) is well matched to the measured profile.

Rain rates of 17.8, 26.0 and 21.2 mm h^{-1} were recorded at the disdrometer sites of NIED (range of 14.7 km), YMTO (21.5 km) and FUSA (27.5 km), respectively at this time and 117.2 mm h^{-1} two minutes later at YMTO. Values of measured reflectivity Z and differential reflectivity Z_{DR} drawn by solid lines in Fig. 2(a) and (c) have already calibration corrected then the differences between measured and corrected values of both reflectivity and differential reflectivity show the significant effect of attenuation along path by rainfall. They reached more than 25 dBZ and 2.5 dB at around 23 km range, respectively. Furthermore the radar signal was missed far from about 26 km range because of strong attenuation by heavy rainfall supposed from the profile of differential propagation phase Φ_{DP} far from 20 km range. It is thought to be the limitation of X-band multiparameter radar MP-X and the longer pulse length or higher power should be adapted particularly for operational use of X-band polarimetric radar. The calculation was ceased at 25 km range because of lower correlation coefficient ρ_{hv} than 0.8.

4.2 Comparisons of Time Series

It is necessary to take into account fundamentally different sampling characteristics of weather radar and disdrometer in comparison between both datasets. The estimates such as rain rates from ZPHI calculations were averaged horizontally within a circle of 2 km radius centered on each disdrometer site using the same bell-shaped weighting function by distance as in Le Bouar et al. (2001). The distance of 2 km corresponds to the scale of the horizontal drift of falling raindrops from 1 km height under the condition of 10 m s^{-1} horizontal wind assuming 5 m s^{-1} terminal velocity of raindrops. The altitudes of radar beam above the disdrometer sites were from 0.7 to 1.2 km. Then both radar and disdrometer estimates were averaged temporally using the same bell-shaped weighting function by time difference with 5-min window width.

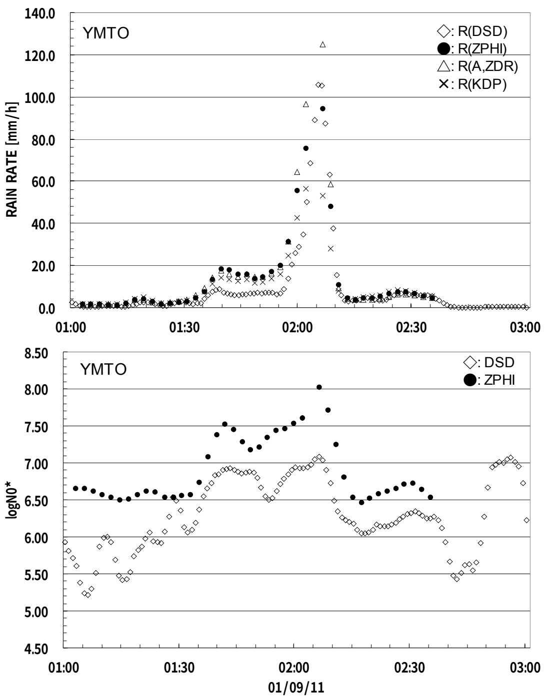

FIG. 3. Comparison of time series of rain rate (upper panel) and normalized intercept parameter (lower panel) among radar estimates and disdrometer measurements at YMTO from 01 to 03 JST on Sep. 11, 2001.

Figure 3 shows time series of the estimated rain rate and estimated normalized intercept parameter N_0^* from radar and disdrometer on YMTO site. This figure shows the results from only the full version of ZPHI algorithm where the difference of Φ_{DP} was larger than 6 deg between both ends of segment and when the quality of retrieval was good that means the root mean square of difference between theoretical and measured Φ_{DP} was less than 8 deg. R(ZPHI), R(A,Z_{DR}) and R(K_{DP}) show the retrieved rain rates from ZPHI algorithm, both estimated specific attenuation A and corrected Z_{DR} by ZPHI algorithm and R-K_{DP} relationship, $R=19.63K_{DP}^{0.823}$, derived from T-matrix calculations based on disdrometer measurements in the DDX01 field experiment and using K_{DP} values not of direct outputs from MP-X but estimated by ZPHI calculation. R(DSD) indicates rain rate estimated from disdrometer measurement in Fig. 3.

The time variations of both rain rate estimates from ZPHI and disdrometers had quite good similarities particularly for high rain rate although the ZPHI estimated rain rates had larger values not only at YMTO but also NIED and FUSA. The reason of the overestimates of rain rate was thought to be the calibration error of the MP-X radar reflectivity because the estimated normalized intercept parameter N_0^* from the radar also showed higher values by about 5 dB (0.5 in $\log N_0^*$) as compared with estimates from disdrometer measurements. This is very probable signification of a wrong calibration of the radar and the effect of the calibration error is estimated in the next section.

It would be suspected that the disdrometer at FUSA had some problems because it was not expected to find a good agreement between radar and disdrometer estimates at FUSA where there was a discrepancy by a factor of two comparing with at NIED and YMTO.

5. DISCUSSIONS

The integrated rainfall amounts from estimated rain rates and average of retrieved normalized intercept parameters were calculated. For these calculations, the estimated rain rates and normalized intercept parameters from the full version of ZPHI algorithm with good calculation quality were used.

All integrated rainfall amounts RA and averages of normalized intercept parameters N_0^* by radar had larger values than that by disdrometers on every disdrometer sites and the differences between them were the larger at the disdrometer site with the longer distance from the radar site. Summarized results for three disdrometer sites indicated in Table 2 show that integrated rainfall amounts RA and averages of normalized intercept parameter N_0^* from ZPHI estimates had about 81 % and 6.2 dB higher values than that from disdrometers. The difference between radar and disdrometer estimates was the largest in RA(A,Z_{DR}) and the smallest in RA(K_{DP}). The overestimates by ZPHI were reduced to about 59 % and 5.9 dB for only NIED and YMTO disdrometers because of extraordinary overestimates on FUSA.

TABLE 2 Integrated rainfall amount RA and averaged normalized intercept parameter N_0^* from radar estimates and disdrometer measurements. ΔRA and $\Delta \log N_0^*$ show the differences between radar estimates and disdrometer measurements. ZPHIcor indicates results after supposed correction of MP-X reflectivity. Averaged values on two disdrometer sites of NIED and YMTO and on all three disdrometer sites are listed.

	NIED & YMTO				3-SITES			
Method	ZPHI	ZPHIcor	A,Z_{DR}	K_{DP}	ZPHI	ZPHIcor	A,Z_{DR}	K_{DP}
RA(RADAR) [mm]	32.9	24.3	34.3	26.6	58.2	43.1	61.8	47.6
RA(DSD) [mm]	20.7	20.7	20.7	20.7	32.1	32.1	32.1	32.1
ΔRA [%]	58.5	17.4	65.6	28.2	81.2	34.3	92.5	43.4
$\log N_0^*$(RADAR)	7.11	6.49			7.13	6.51		
$\log N_0^*$(DSD)	6.51	6.51			6.51	6.51		
$\Delta \log N_0^*$ [dB]	5.94	-0.26			6.19	-0.01		

The difference of 6.2 dB as averaged between normalized intercept parameter N_0^* derived from the radar and the disdrometers in Table 2 implies a radar calibration error of -1.9dB and an impact on rain rate R(ZPHI) can be estimated by the factor 1/1.35 (Le Bouar et al., 2001). The estimated calibration correction resulted in values in the columns of the ZPHIcor in Table 2. After this correction, the bias of RA(ZPHI) was quite small by about 10 and 22 % with NIED and YMTO disdrometers and acceptable but that with FUSA remained showing a big overestimation of 65 %. In all cases after the correction, RA(ZPHIcor) improved better than RA(K_{DP}) using R-K_{DP} relationship. The bias of RA(ZPHIcor) and RA(K_{DP}) averaged at two disdrometer sites of NIED and YMTO was about 17 and 28 %, respectively.

6. CONCLUSIONS

The rain profiling algorithm ZPHI developed by Testud et al. (2000) was applied to the rainfall data collected in the field experiment using an X-band multiparameter radar MP-X of the National Research Institute for Earth Science and Disaster Prevention (NIED) and three impact type disdrometers around Tsukuba city, Japan from August 8 to October 4 in 2001.

The estimated rain rate and normalized intercept parameter N_0^* from ZPHI algorithm were compared with the disdrometer measurements during the rainfall period associated with Typhoon T0115 when the maximum rain rate of 121 mm h^{-1} was recorded on the ground. Time variations of both rain rates estimated from ZPHI and disdrometers had quite good similarities although the radar estimated rainfall amount had larger values by about 80 %. The reason of the overestimates was thought to be the calibration error of the MP-X radar reflectivity because the estimated N_0^* from the radar also showed higher values than ones estimated from disdrometer measurements.

The calibration correction of -1.9 dB was supposed from the bias of estimated normalized intercept parameter N_0^*. After the correction by using the supposed reflectivity calibration correction, the bias of RA(ZPHI) improved to 17 % better than the bias of 28 % of RA(K_{DP}) with respective to two disdrometer sites in this rainfall case.

In order to examine our guess and for more accurate rain rate estimations, the radar calibration correction should be estimated from both examining statistics of N_0^* in detail and consistency test between the rain rate estimate by ZPHI and the estimate combining specific attenuation A and differential reflectivity Z_{DR}, and applied hereafter. Also increasing calculation cases should be done in order to validate ZPHI algorithm in application to X-band polarimetric radars.

ACKNOWLEDGEMENTS

This study was conducted in the framework of the joint research contract of “Evaluation, test and validation of algorithm ZPHI applied to X-band radar data” between CETP-CNRS, UVSQ and NIED. Authors wish to acknowledge coding some programs for data transformation of NIED MP-X data to the input format for ZPHI calculations by Dr. David Weissenbach.

REFERENCES

Bringi, V. N., V. Chandrasekar, N. Balakrishnan and D. S. Zrnić, 1990: An examination of propagation effects in rainfall on polarimetric variables at microwave frequencies. *J. Atmos. Oceanic Tech.*, **7**, 829-840.

Iwanami, K., R. Misumi, M. Maki, S. Watanabe, K. Hata, Wakayama, 2001: Development multiparameter radar system on mobile platform. *Proc. 30th Intern'l Conf. Radar Meteor., July 2001, Munich, Germany*, 104-106.

Gorgucci, E., G. Scarchilli and V. Chandrasekar, 1999: A procedure to calibrate multiparameter weather radar using properties of the rain medium. *IEEE Transactions Geosci. Remote Sensing*, **37**, 269-276.

Le Bouar, E., J. Testud and T. D. Keenan, 2001: Validation of the rain profiling algorithm “ZPHI” from the C-band polarimetric weather radar in Darwin. *J. Atmos. Oceanic Tech.*, **18**, 1819-1837.

Le Bouar, E, J. Testud and S. Y. Matrosov, 2002: Rainfall rate estimate from the rain profiling algorithm “ZPHI” applied to X-band polarimetric radar data. *Proc. European Conf. Radar Meteor., November 2002*, *Delft, Netherlands,* 238-242.

Testud, J., S. Oury, R. A. Black, P. Amayenc and X. Dou, 2001: The concept of ”normalized” distribution to describe raindrop spectra: A tool for cloud physics and cloud remote sensing. *J. Appl. Meteor.*, **40**, 1118-1140.

Testud, J., E. Le Bouar, E. Obligis and M. Ali-Mehenni, 2000: The rain profiling algorithm applied to polarimetric weather radar. *J. Atmos. Oceanic Tech.*, **17**, 332-356.